2015 American Control Conference
Palmer House Hilton
July 1-3, 2015. Chicago, IL, USA

Coordinated Active Steering and Four-wheel Independently Driving/Braking Control with Control Allocation

Jinxiang Wang[1], Rongrong Wang[1], Hui Jing[1], Mohammed Chadli[2], and Nan Chen[1]

Abstract— **This paper presents a hierarchical coordinated control algorithm for integrating active front steering and four-wheel independently driving/braking control. In the higher-level controller, an adaptive siding mode control law and a coordination law for adjusting the yaw rate and slip angle control priorities are applied to determine the desired front wheel steering angle and external yaw moment. In the lower-level controller, a control allocation algorithm with actuators and tire forces constraint considerations is designed to assign the desired yaw moment to the front wheel steering system and four wheels. The weighting factors of tracking errors and control inputs in the cost function are online updated according to the vehicle stability index. Simulation results with a high-fidelity, CarSim, full-vehicle model show that handling and stability of the vehicle can be improved with the proposed controller. What is more, control of sideslip angle can be more focused when the vehicle is hitting the manoeuvring limitation.**

I. INTRODUCTION

Compared to conventional centralized driven vehicles with mechanical drivetrains, electric ground vehicles driven by four independently actuated in-wheel motors have much better performance in terms of stability and energy efficiency, thanks to independently control of driving/braking torque of each wheel and the fast yet precise responses of electric motors [1]. On the other hand, steer-by-wire systems hold advantages over traditional automotive steering systems on handling behavior during normal driving and stability maintenance during critical driving.

The control of active steering and active driving/braking systems for better handling and preventing of drift has been actively studied [2]. Active steering control is effective for improving vehicle handling characteristics and can maintain vehicle stability by generating contra-cornering yaw moment near the limitation of tire road adhesion through reducing the steering angle [3][4][5]. But under severe manoeuvres when the vehicle is very close to the handling limit, active steering control becomes inefficient in following the desired yaw rate, while variable torque distribution (VTD) control has considerable effects on yaw moment and lateral acceleration [6]. Brake force distribution (BFD) including differential braking are more effective than active front-wheel steering (AFS) and VTD in tracking yaw rate and bounding sideslip in the condition of handling limit [7]. Although having best capacity for yaw tracking and stability, the BFD may severely influence the longitudinal performance [2]. For the electric ground vehicle with four independently actuated in-wheel motors [1][8], differential driving/braking can be easily realized to produce the desired corrective yaw moment (can be denoted as direct yaw moment control, DYC) while maintaining demanded longitudinal motion. What is more, if the consumption of motor energy is considered, combined use of active steering and four-wheel independently driving/braking system will have better global performance [9].

It was reported that the multi-layer control architecture is more effective and flexible for coordinating vehicle subsystems [10]. With this architecture, the global control efforts of desired yaw moment and total tire forces are calculated by the higher-level controller, while these efforts are assigned to corresponding actuators in the lower level. The higher-level control algorithms which integrate AFS and DYC for enhancing maneuvering performance and reducing accidents were studied recently in [11][12][13][14]. Methods of assigning the global control efforts to the lower-level actuators can be categorised to rule based [12][13][15] and optimization based control allocation [14][16][17][18][19]. The main advantages of control allocation compared with the rule based methods are the capability of considering multiple control objectives and constraints of actuators, and maximizing the potential of tire forces and reconfigurability during the failure of some actuators. Among the optimization based allocation algorithms used in literatures, weightings of the multiple control objectives were preset and remained unchanged throughout the maneuvering scenarios. But in practice, the importance of tracking desired yaw motion and maintaining stability will be transferred due to the change of vehicle states such as criticality of stability.

In this paper, a hierarchical control structure is applied. In the higher-level controller, an adaptive siding mode control law and a coordination weighting law are applied to determine the desired front wheel steering angle and the desired yaw moment. In the lower-level controller, a control allocation method with input saturations and rate limit considerations is implemented to allocate the desired control signals to each actuators. The weighting factors of tracking errors and control inputs in the cost function are updated online according to the proposed stability index. The rest of this paper is organised as follows. In Section 2, a simplified linear vehicle model is presented. Section 3 gives the design procedure of the adaptive sliding mode controller, followed by the implementation of control allocation in the lower-level

*This work was supported by National Natural Science Foundation of China (Grant No. 51205058, 51375086).

[1]Jinxiang Wang, Rongrong Wang, Hui Jing, and Nan Che are with School of Mechanical Engineering, Southeast University, Nanjing 211189, P.R. China. e-mail: wangjx@seu.edu.cn, wrr06fy@gmail.com, jinghuiguet@gmail.com, nchen@seu.edu.cn.

[2]Mohammed Chadli is with the University of Picardie Jules Verne, MIS (E.A. 4290). 80039, Amiens, France.e-mail: mohammed.chadli@u-picardie.fr

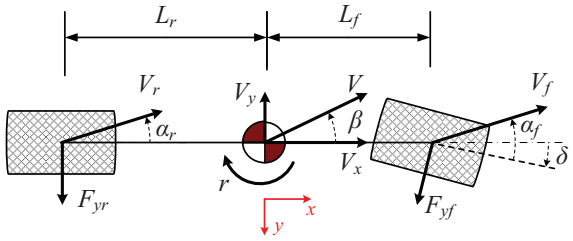

Fig. 1. A 2DOF vehicle model.

controller in section 4. Simulation based on a high-fidelity, CarSim, full-vehicle model are shown in Section 5 followed by conclusive remarks.

II. System Modelling

A. Vehicle Model

Assuming the left and right tires have the same steering angles and slip angles, the vehicle lateral plane motions can be represented with a bicycle vehicle model which is as Fig.1 shows. The vehicle model can be described as [3],

$$\begin{cases} \dot{\beta} = \frac{-2(C_f+C_r)}{mV_x}\beta + \left(\frac{2(C_fL_f-C_rL_r)}{mV_x^2}+1\right)r \\ \quad + \frac{2C_f}{mV_x}\delta + d_1 \\ \dot{r} = \frac{2(C_rL_r-C_fL_f)}{I_z}\beta - \frac{2(C_fL_f^2+C_rL_r^2)}{I_zV_x}r \\ \quad + \frac{2C_fL_f}{I_z}\delta + \frac{M_{zc}}{I_z} + d_2 \end{cases} \tag{1}$$

where I_z is the vehicle inertia along the z-axis, r is the yaw rate, β is the vehicle sideslip angle, C_f and C_r are values of the front and rear tire cornering stiffness, respectively, d_1 and d_2 are external disturbances, M_{zc} is the external yaw moment generated with the tire force differences between two sides of the vehicle and can be defined as,

$$M_{zc} = \frac{l_s}{2}(F_{xfl} - F_{xfr} + F_{xrl} - F_{xrr}), \tag{2}$$

where l_s is the track width. Let

$$M_z = M_{zc} + 2C_fL_f\delta, \tag{3}$$

where the second term of M_z is the yaw moment induced by the front wheel steering angle δ, the vehicle model can be rewritten as

$$\dot{x} = Ax + Bu + d, \tag{4}$$

where

$$x = \begin{bmatrix} \beta \\ r \end{bmatrix}, \quad u = \begin{bmatrix} \delta \\ M_z \end{bmatrix}, \quad d = \begin{bmatrix} d_1 \\ d_2 \end{bmatrix},$$

$$A = \begin{bmatrix} -2\frac{C_f+C_r}{mV_x} & \frac{2(C_rL_r-C_fL_f)}{mV_x^2} - 1 \\ \frac{2(C_rL_r-C_fL_f)}{I_z} & \frac{-2\left(C_fL_f^2+C_rL_r^2\right)}{I_zV_x} \end{bmatrix},$$

$$B = \begin{bmatrix} \frac{2C_f}{mV_x} & 0 \\ 0 & \frac{1}{I_z} \end{bmatrix}.$$

III. Sliding Mode Controller Design

A. Reference Generation

The control objective is to track the desired yaw rate with upper bound while restraining the vehicle side slip in a reasonable range. The desired yaw rate can be given by an empirical pre-filtered transfer function as [3]

$$r_{des} = \frac{G_{ss}(V_x)}{0.1s+1}\delta_d, \tag{5}$$

where δ_d is the steering angle given by the driver, G_{ss} is defined as

$$G_{ss}(V_x) = \frac{V_x}{L + m\frac{C_rL_r-C_fL_f}{2C_fC_r(L_f+L_r)}V_x^2}. \tag{6}$$

According to the two degrees of freedom vehicle model and under the assumption of small vehicle side slip angle and side slip angle rate, the vehicle yaw rate is bounded as [20],

$$|r| \le r_{limt} = (1-\theta)\frac{\sqrt{\mu^2g^2 - a_x^2}}{V_x}, \tag{7}$$

where μ is the tire road friction coefficient (TRFC), θ is a positive constant denoting the influence of vehicle side slip angle. Thus, the control target of yaw rate tracking is given by

$$r_{tg} = r_{limt}sat\left(\frac{r_{des}}{r_{limt}}\right), \tag{8}$$

where the saturation function is defined as

$$sat(x) = \begin{cases} -1, & x \le -1 \\ x, & -1 < x < 1 \\ 1, & x \ge 1 \end{cases}. \tag{9}$$

The vehicle sideslip angle must also be bounded to ensure handling stability, with empirical relation as follows

$$|\beta| < \beta_{limt}, \tag{10}$$

with $\beta_{limt} = 0.02\mu g$. This agrees with the desirable upper bound of slip angle on both high and low friction coefficient road [21].

B. Adaptive Sliding Mode Controller Design

Vehicle system is an intrinsic highly nonlinear system, controllers designed with a linear model cannot handle model uncertainties and external disturbances within a wide range. In order to improve robustness with respect to vehicle system parametric uncertainties and disturbance, an adaptive sliding mode controller is designed to calculate the desired yaw moment and front wheel steering angle. Define the sliding mode surface as,

$$s = x - x_{tg}, \tag{11}$$

where $x_{tg} = [r_{tg} \quad \beta_{tg}]^T$ with β_{tg} being the vehicle slip angle reference. The reaching law of the sliding mode control can be described as

$$\dot{s} = -\Lambda s - H\dot{s} - K(t)sign(s), \tag{12}$$

with $\Lambda = diag(\lambda_1, \lambda_2)$, $H = diag(\eta_1, \eta_2)$, and $K = diag(\kappa_1, \kappa_2)$, being positive definite matrices ensure the global stability of the sliding mode control system.

$Proof$: Define a Lyapunov function as

$$V = \frac{1}{2} s^T s. \tag{13}$$

Evaluating the time derivative of (13), we have

$$\begin{aligned} \dot{V} &= s^T \dot{s} \\ &= s^T \left(I + H^T\right)^{-1} \left(-\Lambda s - K(t) sign(s) + d\right) \\ &= -(I + H)^{-1} \left(\Lambda s^T s + K(t) s^T sign(s) - s^T d\right) \end{aligned} \tag{14}$$

Since $(I + H) = diag(1 + \eta_1, 1 + \eta_2)$ is positive definite, $(I + H)^{-1}$ is positive definite. If $s \neq 0$ and the disturbance is upper bounded, then $s^T s > 0$ and $s^T sign(s) > 0$, and by choosing $K(t)$ to be sufficiently large, $K(t) s^T sign(s) > s^T d$ can be satisfied. Thus $\dot{V} < 0$, and global stability of the sliding mode control system is guaranteed.

In the reaching law of the sliding mode control (12), the matrix Λ defines the converge speed of s, and $H\dot{s}$ is applied to reduce the overshoot of the tracking response. In order to eliminate chattering due to the change of structural parameters and external disturbance, we replace $sign(s)$ with the saturation function $sat\left(E^{-1}s\right)$, where $E = diag(\varepsilon_1, \varepsilon_2)$ is the border dense denoting the steady state error tolerance. The control gain $K(t)$ can be adjusted by the following adaptation law [22],

- If $|s| > \epsilon > 0$, $K(t)$ is solution of the following differential equation

$$\dot{K}(t) = \bar{K}_1 |s|, \tag{15}$$

  with $\bar{K}_1 > 0$ and $K(0) > 0$;
- If $|s| < \epsilon$, then

$$\begin{cases} K(t) = \bar{K}_2 |\rho(t)| + \bar{K}_3 \\ \tau \dot{\rho}(t) + \rho(t) = sat\left(E^{-1}s\right) \end{cases} \tag{16}$$

  with $\bar{K}_2 = K(t^*)$, $\bar{K}_3 > 0$ and $\tau > 0$, where t^* is the instant when $|s|$ hitting the border ϵ.

According to the adaptation law (15), the control gain $K(t)$ will increase to a value which is large enough to set-off the bounded parameter uncertainties and disturbances, thus the occurrence of the sliding mode is guaranteed. According to the adaptation law (16), the control gain $K(t)$ is allowed to be decreased and adjusted according to the current uncertainties and perturbations when the sliding mode starts.

By collecting model (4), the sliding surface and reaching law, the sliding mode control signals can be given by

$$\begin{aligned} u^{des} &= \begin{bmatrix} \delta_\beta^{des} & M_z^{des} \end{bmatrix}^T \\ &= B^{-1} \big[-\Lambda s - H\dot{s} - K(t) sat\left(E^{-1}s\right) \\ &\quad - Ax - \dot{x}_{tg} \big]. \end{aligned} \tag{17}$$

The control input δ_β^{des} is designed to constrain β within a reasonable range to avoid the risk of vehicle slip, while M_z^{des} is used to track r_{tg}. Note that AFS can also be used in yaw rate control, and have been confirmed very effective in small and medium a_y condition[5]. However, when the vehicle state is hitting the manoeuvring limitation, AFS may become inefficient in tracking of the yaw rate. Although AFS is still available to achieve some contra-cornering yaw moment, restricting β from being uncontrollable, it is actually not able to regulate β back to zero when a_y is around its limitation.

Considering tire force and sideslip limitation, the stability index is defined as

$$C_{SI} = \frac{1}{2} \sqrt{\frac{|\beta + w_1 \dot{\beta}|^2}{\beta_{limt}^2} + \frac{a_x^2 + a_y^2}{\mu^2 g^2}} \tag{18}$$

where w_1 denotes the contribution of $\dot{\beta}$ to the instability, then by considering both yaw rate and sideslip control targets, compromised control considering vehicle stability can be obtained. The control law is modified as

$$\begin{cases} \delta_\beta^c = \overline{sat}\left(\frac{C_{SI} - \xi_1}{\sigma_1}\right)\left(\delta_\beta^{des} - \delta_d\right) \\ \overline{M}_z^{des} = \overline{sat}\left(\frac{\xi_2 - W_\beta}{\sigma_2}\right) M_z^{des} \end{cases} \tag{19}$$

where δ_β^c is the corrective steering angle for sideslip control, ξ_i and $\sigma_i, (i = 1,\ 2)$ are preselected positive constants, W_β and $\overline{sat}(x)$ are defined as

$$W_\beta = \overline{sat}\left(\frac{C_{SI} - \xi_1}{\sigma_1}\right) \tag{20}$$

$$\overline{sat}(x) = \begin{cases} 0, & x \leq 0 \\ x, & 0 < x < 1 \\ 1, & x \geq 1 \end{cases}. \tag{21}$$

It can be observed from (19) that when C_{SI} is small, the sideslip control is disabled, both front wheel steering regulation and M_{zc} are employed for yaw rate control; when C_{SI} becomes large, the weighting for M_z^{des} is decreased and front tire steering regulation is used for generating contra-cornering yaw moment to reduce sideslip angle.

With Eq. (3), the modified yaw moment is implemented by desired δ for yaw rate tracking control and desired M_{zc} as follows

$$\overline{M}_z^{des} = M_{zc}^{des} + 2C_f L_f \delta_{yaw}^{des} \tag{22}$$

where M_{zc}^{des} is generated by the four longitudinal tire forces. The allocation of $\overline{M}_z^{des}$ to tire forces and steering angle will be presented in following section.

IV. Control Allocation Design

The tracking errors of both yaw rate and longitudinal acceleration must be minimized to achieve better control performance, meanwhile the control inputs needs to be minimized to avoid the nonlinear limit region of tire forces. Thus the cost function can be defined as follows

$$J(v) = e^T Q e + v^T R v, \tag{23}$$

where

$$e = \begin{bmatrix} e_1 & e_2 \end{bmatrix}^T,$$

$$e_1 = F_{xfl} + F_{xfr} + F_{xrl} + F_{xrr} - f_r mg - ma_x^{des},$$

$$
\begin{aligned}
e_2 &= \frac{L_w}{2}\left(F_{xfl} - F_{xfr} + F_{xrl} - F_{xrr}\right) \\
&\quad + 2C_f L_f \delta_{yaw}^{des} - \overline{M}_z^{des}, \\
v &= \left[F_{xfl}\ F_{xfr}\ F_{xrl}\ F_{xrr}\ \delta_{yaw}^{des}\right]^T, \\
Q &= diag\left(w_{a_x}, w_{yaw}\right), \\
R &= diag\left(\frac{w_x}{F_{zfl}^2}, \frac{w_x}{F_{zfr}^2}, \frac{w_x}{F_{zrl}^2}, \frac{w_x}{F_{zrr}^2}, w_\delta\right).
\end{aligned}
$$

e_1 and e_2 are tracking errors of yaw rate and longitudinal acceleration, respectively, the vector v represents the actual control efforts from the actuators. $F_{zi}(i = fl, fr, rl, rr)$ is vertical load on each wheel, which can be estimated on each control step, w_{a_x}, w_{yaw}, w_x and w_δ are weighting factors of tracking errors and each actuators, these weighting factors are functions of the stability index and can be written as,

$$
\begin{cases}
w_{ax} = w_{ax0}\left[1 - \overline{sat}\left(\dfrac{C_{SI}}{\sigma_3}\right)\right] \\
w_{yaw} = w_{yaw0}\left[1 - \overline{sat}\left(\dfrac{C_{SI}}{\sigma_4}\right)\right] \\
w_x = w_{x0}\left[1 + \dfrac{C_{SI}}{\sigma_5}\right] \\
w_\delta = w_{\delta 0}\left[1 + \dfrac{C_{SI}}{\sigma_6}\right] + w_{\delta 1} W_\beta^2
\end{cases}
$$

where w_{ax0}, w_{yaw0}, w_{x0} and $w_{\delta 0}$ are initial weighting factors when the stability index is zero, $\sigma_i(i = 3, ..., 6)$ are positive constants. $w_{\delta 1}$ is chosen to be a large positive constant such that the steering input for yaw rate control can be disabled when the sideslip controller is activated.

In practical, the actual control efforts v is constrained by tire-road adhesion limit and rate limits of motors and hydraulic brake actuators which can be represented as

$$
\begin{cases}
\frac{F_{xi}^2}{F_{zi}^2} + \frac{F_{yi}^2}{F_{zi}^2} \le \mu_i^2 \\
F_{min} \le F_{xi} \le F_{max} \\
\delta_{min} \le \delta_{yaw}^{des} \le \delta_{max} \\
F_{min}^{rt} \le F_{xi}(t + \Delta t) - F_{xi}(t) \le F_{max}^{rt} \\
\delta_{min}^{rt} \le \delta_{yaw}^{des}(t + \Delta t) - \delta_{yaw}^{des}(t) \le \delta_{max}^{rt}
\end{cases}
\tag{24}
$$

where μ_i is the TRFC of the ith tire, and Δt is time step of the optimizing controller. On each time step, F_{yi} and F_{zi} are estimated with the current vehicle states, the control inputs of last step are used to calculate the constraints of rate limits. Thus the constraints (24) can be rewritten as $g_j(v) \ge 0, (j = 1, ..., 24)$, and the optimization problem with inequality constraint can be defined as

$$
\begin{aligned}
&\min \quad J(v) \\
&s.t. \quad g_j(v) \ge 0, (j = 1, ..., 24)
\end{aligned}
\tag{25}
$$

The augmented lagrangian method [23][24][25] has the property of superior convergence, much easier to regulate parameters, and is able to find the optimal solution without penalty factors which approach to infinity. In this paper, the algorithm of augmented Lagrange multipliers is introduced to solve the optimization problem with inequality constraints.

The optimization problem (25) in the form of augmented lagrangian function can be written as

$$
\begin{aligned}
\min\ \phi(v, w, \sigma_7) &= J(v) \\
&+ \frac{1}{2\sigma_7}\sum_{j=1}^{24}\left\{\left[\max\left(0, w_j - \sigma_7 g_j(v)\right)\right]^2 - w_j^2\right\}
\end{aligned}
\tag{26}
$$

where σ_7 is the penalty factor. The multipliers $w^{(k+1)}$ in the $(k+1)$th iteration can be updated using w^k in the kth iteration, with the following updating law

$$
w_j^{(k+1)} = \max\{0, w_j^k - \sigma_7 g_j\left(v^k\right)\}, j = 1, ..., 24 \tag{27}
$$

The initial value of σ_7 must be a positive parameter large enough, and can be updated with following procedure

$$
\begin{aligned}
h_j(v) &= g_j(v) - \frac{1}{\sigma_7}\max\{0, \sigma_7 g_j(v) - w_j\}, j = 1, ..., 24 \\
\vartheta^k &= \begin{cases}
0, & \dfrac{||h\left(v^k\right)||}{||h\left(v^{(k-1)}\right)||} < \varphi \\
1, & \dfrac{||h\left(v^k\right)||}{||h\left(v^{(k-1)}\right)||} \ge \varphi
\end{cases} \\
\sigma_7^{(k+1)} &= \sigma_7^k + \vartheta^k(\zeta - 1)\sigma_7^k
\end{aligned}
$$

where $\varphi \in (0, 1)$ and $\zeta > 1$ are constant parameters.

The unconstrained optimization problem can be solved with trust region method [26]. In order to calculate the gradient vector and Hessian matrix of $\phi(v, w, \sigma_7)$, problem (26) can be reformulated as

$$
\begin{aligned}
\min \quad & \phi(v, w, \sigma_7) = J(v) + \\
& \frac{1}{2\sigma_7}\left[\left(w - \sigma_7 g(v)\right)^T P\left(w - \sigma_7 g(v)\right) - w^T w\right]
\end{aligned}
\tag{28}
$$

where $P = diag(p_1, ..., p_{24})$ can be determined in each iteration as

$$
p_j^k = \begin{cases}
0, & w_j^k - \sigma_7 g_j(v^k) \le 0 \\
1, & w_j^k - \sigma_7 g_j(v^k) > 0
\end{cases} \quad j = 1, ..., 24 \tag{29}
$$

V. SIMULATION AND RESULTS

In order to verify the performance of the adaptive sliding mode controller and control allocation algorithm proposed in this paper, simulation results with a high-fidelity, CarSim, full-vehicle model is conducted. In the simulation, the vehicle had an initial velocity of $50\mathrm{km \cdot h^{-1}}$, the TRFC was set to 0.5, and the desired longitudinal acceleration was $2.5\mathrm{m \cdot s^{-2}}$ throughout the simulation. A counter-clockwise turn which made the hand wheel steering angle finally maintained at 3.5 degree was applied at 2.0s. The desired yaw rate was upper bounded by (7), in which θ was taken as 0.15. Performance of the vehicle with the proposed control algorithm was compared with the one without control, with which the longitudinal forces assigned to the four tires were equivalent and the driver's steering input was applied directly to the front axle.

The vehicle yaw rates and accelerations are shown in Figure 2(a) and Figure 2(c), respectively. Under the condition of intented steering input and longitudinal acceleration from the driver, the desired yaw rate had grown bigger than the

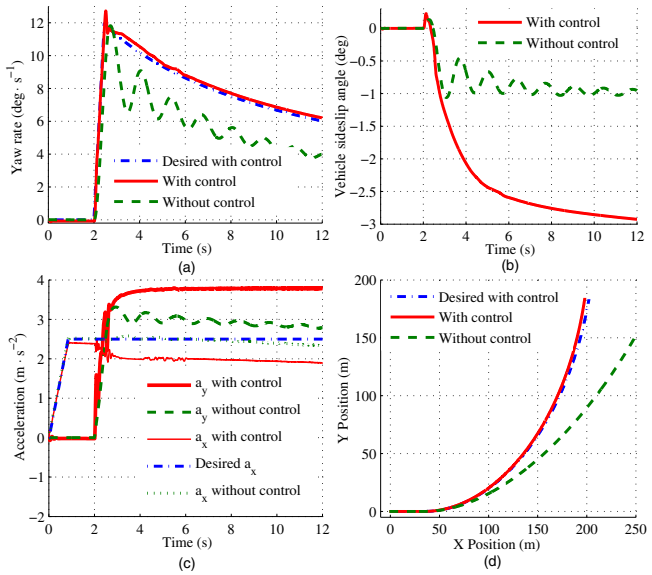

Fig. 2. Vehicle body response in the simulation.

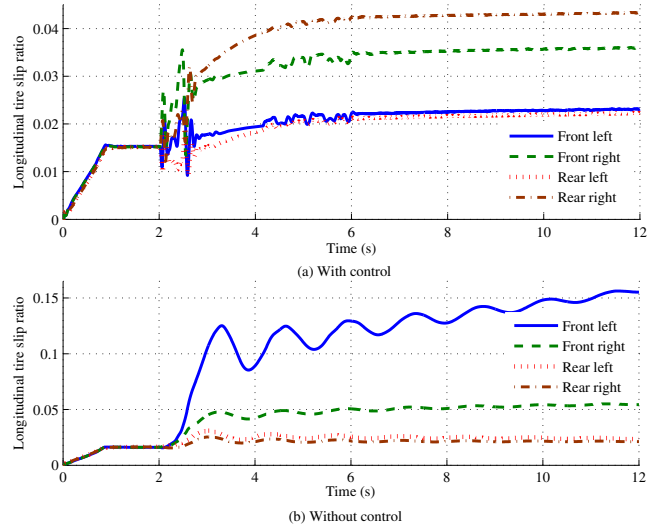

Fig. 3. Longitudinal tire slip ratio in the simulation.

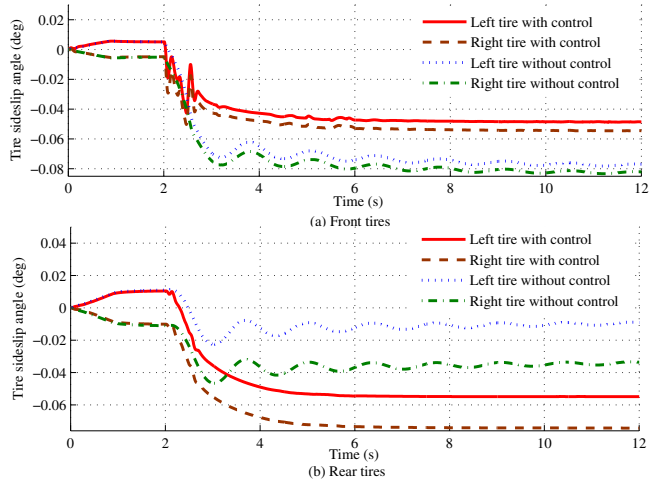

Fig. 4. Tire sideslip angle in the simulation.

upper bound, i.e. $r_{des} > r_{limt}$. The controlled longitudinal acceleration was maintained approximately at $2.0\mathrm{m}\cdot\mathrm{s}^{-2}$ as the vehicle speed kept increasing, r_{limt} was decreasing as described in (7), making the control target of yaw rate decreased due to (8), as shown in Figure 2 (a). It also can be observed that the controlled yaw rate can track the reference well, while the yaw rate without control shows tremendous understeer. As a result, the controlled vehicle can follow the desired trajectory well, while the vehicle without control had slipped off the desired curve due to serious understeer, as shown in Figure 2 (d). Note that a_x and $\sum \frac{F_{xi}^2}{F_{zi}^2}, (i = fl, fr, rl, rr)$ of the controlled vehicle were directly influenced by the values of w_{a_x} and w_x in the cost function (23). More specifically, the increase of w_x reduced the value of $\sum \frac{F_{xi}^2}{F_{zi}^2}$, leading to smaller vehicle sideslip, but on the other hand it also resulted in the reduction of $\sum F_{xi}$, thus a_x approximately decreased by $0.5\mathrm{m}\cdot\mathrm{s}^{-2}$, as Figure 2 (c) shows.

For the controlled vehicle, it is shown in Figure 2(c) that lateral acceleration was stabilized at $3.8\mathrm{m}\cdot\mathrm{s}^{-2}$, resulting in a resultant planar acceleration of $4.3\mathrm{m}\cdot\mathrm{s}^{-2}$ which was 0.86 times of μg. This implies that the vehicle was near the critical condition. Note that the longitudinal and lateral slips were still in stable regions in this case. The vehicle sideslip angle was settled down at a medium situation, about 2.9 degree as shown in Figure.2(b), and both longitudinal tire slip ratio and lateral tire sideslip angle were constrained in stable region avoiding large side slip or spinning, as shown in Figure 3 and Figure 4. As for the vehicle without control, although the vehicle sideslip angle was smaller than the one with control, both of the longitudinal slip ratio and the sideslip angle of front tires were quite larger than the rear tires. What is more, the longitudinal slip ratios of front left tires were larger than 0.14 and kept increasing with oscillating, resulting in severe understeer of the vehicle.

Figure 5(a) shows that the longitudinal forces assigned to tires was approximately proportional to their vertical forces for minimizing the second part of the cost function, i.e. $v^T Rv$, before the J-turn was applied. After the J-turn was applied, yaw rate tracking error was added to the cost function, the allocation of tire forces became more complicated. The stability index of the controlled vehicle was not larger than the threshold ξ_1 in the simulation, so the steering control was used only for generating yaw moment M_z, and the corrective steering angle for sideslip control was disabled. In this case, tire forces in the outer side were larger than those in the inner side for minimizing $v^T Rv$. Figure 6 shows that the yaw moment M_{zc} in the direction of driver's steering was generated to release the demand of steering angle, thanks to the tire force difference. Thus the front wheel steering and longitudinal tire forces were coordinated to generate direct yaw moment M_{zc} and indirect yaw moment equivalent to the second part of (3), adding these two contributions of yaw moment well generates the desired M_z which is as Figure 6 shows.

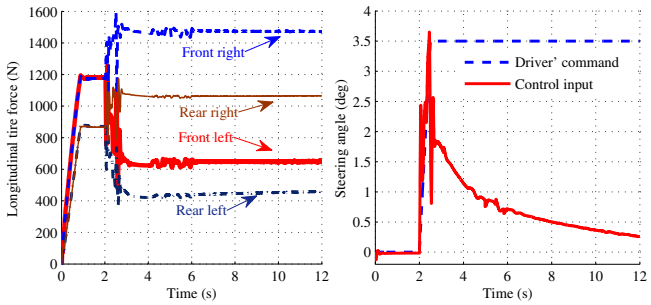

Fig. 5. Controller input in the simulation.

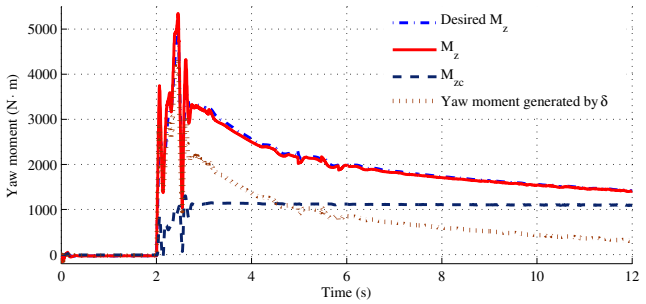

Fig. 6. Yaw moment in the simulation.

VI. Conclusion

In this paper, an adaptive siding mode control law and a coordination weighting law based on the vehicle stability index are designed to determine the desired front wheel steering angle and corrective yaw moment in the higher-level controller. The coordination weighting law is designed to transfer the control priority between tracking desired yaw motion and maintaining stability according to the change of vehicle states such as criticality of stability. In the control allocation, the weighting factors of the tracking errors and control inputs in the cost function are updated online according to the vehicle stability index. Simulation results show that the tracking of desired yaw rate and maintaining reasonable sideslip can be well adjusted according to the vehicle actual states. The overall performance of handling and stability is thus improved.

References

[1] R. Wang, Y. Chen, D. Feng, X. Huang, and J. Wang, "Development and performance characterization of an electric ground vehicle with independently actuated in-wheel motors," *Journal of Power Sources*, vol. 196, no. 8, pp. 3962-3971, 2011.

[2] W. J. Manning and D. A. Crolla, "A review of yaw rate and sideslip controllers for passenger vehicles," *Transactions of the Institute of Measurement and Control*, vol. 29, no.2, pp. 117-135, 2007.

[3] J. Ackermann, "Robust control prevents car skidding," *IEEE Control Systems*, vol. 17, no. 3, pp. 23-31, 1997.

[4] P. Yih and J. C. Gerdes, "Modification of vehicle handling characteristics via steer-by-wire". *IEEE Transactions on Control Systems Technology*, vol. 13, no. 6, pp. 965-976, 2005.

[5] J. He, D. A. Crolla, M. C. Levesley, and W. J. Manning, "Integrated active steering and variable torque distribution control for improving vehicle handling and stability," *SAE transactions* , vol. 113, No. 6, pp.638-647, 2004.

[6] R. P. Osborn and T. Shim, "Independent control of all-wheel-drive torque distribution," *Vehicle System Dynamics*, vol. 44, no. 7, pp. 529-546, 2006.

[7] M. Jonasson, J. Andreasson, B. Jacobson, and A. S. Trigell. "Global force potential of over-actuated vehicles," *Vehicle System Dynamics*, vol. 48, no. 9, pp. 983-998, 2010.

[8] R. Wang, H. Zhang, and J. Wang, "Linear parameter-varying controller design for four-wheel independently actuated electric ground vehicles with active steering systems," *IEEE Transactions on Control Systems Technology*, vol. 22, no. 4, pp. 1281-1296, 2013.

[9] Y. Chen and J. Wang, "Fast and global optimal energy-efficient control allocation with applications to over-actuated electric ground vehicles," *IEEE Transactions on Control Systems Technology*, vol. 20, no. 5, pp. 1202-1211, 2012.

[10] T. Gordon, M. Howell, and F. Brandao. "Integrated control methodologies for road vehicles," *Vehicle System Dynamics*, vol. 40, nos. 1-3, pp. 157-190, 2003.

[11] S. Di Cairano, H. E. Tseng , D. Bernardini, and A. Bemporad, "Vehicle yaw stability control by coordinated active front steering and differential braking in the tire sideslip angles domain," *IEEE Transactions on Control Systems Technology*, vol.21, no. 4, pp. 1236-1248, 2013.

[12] J. He, D. A. Crolla, M. C. Levesley, and W. J. Manning, "Coordination of active steering, driveline, and braking for integrated vehicle dynamics control," *Proceedings of the Institution of Mechanical Engineers, Part D: Journal of Automobile Engineering*, vol. 220, no. 10, pp. 1401-1420, 2006.

[13] M. Doumiati, O. Sename, L. Dugard, J. J. Martinez-Molina, P. Gaspar, and Z. Szabo, "Integrated vehicle dynamics control via coordination of active front steering and rear braking," *European Journal of Control*, vol. 19, no. 2, pp. 121-143, 2013.

[14] T. Weiskircher and S. Mller, "Control performance of a road vehicle with four independent single-wheel electric motors and steer-by-wire system," *Vehicle System Dynamics*, vol. 50, no. sup 1, pp. 53-69, 2012.

[15] K. R. Buckholtz, "Use of fuzzy logic in wheel slip assignment - part I: yaw rate control," *SAE World Congress*, no. 2002-01-1221, 2002.

[16] O. Mokhiamar and M. Abe, "Simultaneous optimal distribution of lateral and longitudinal tire forces for the model following control," *Journal of dynamic systems, measurement, and control*, vol. 126, no. 4, pp. 753-763, 2004.

[17] J. Wang and R. G. Longoria, "Coordinated and reconfigurable vehicle dynamics control," *IEEE Transactions on Control Systems Technology*, vol. 17, no. 3, pp. 723-732, 2009.

[18] M. Jonasson, J. Andreasson, S. Solyom, B. Jacobson, and A. S. Trigell, "Utilization of actuators to improve vehicle stability at the limit: From hydraulic brakes toward electric propulsion," *Journal of Dynamic Systems, Measurement, and Control*, vol. 133, no. 5, p. 051003, 2011.

[19] T. A. Johansen and T. I. Fossen, "Control allocation - a survey," *Automatica*, vol. 49, no. 5, pp. 1087-1103, 2013.

[20] J. X. Wang, N. Chen, D. W. Pi, and G. D. Yin. "Agent-based coordination framework for integrated vehicle chassis control," *Proceedings of the Institution of Mechanical Engineers, Part D: Journal of Automobile Engineering*, vol. 223, no. 5, pp. 601-621, 2009.

[21] A. T. Van Zanten, R. Erhardt, and G. Pfaff, "VDC, the vehicle dynamics control system of Bosch," *SAE Technical Paper*, no. 950759, 1995.

[22] V. I. Utkin, A. S. Poznyak, "Adaptive Sliding Mode Control," *Advances in Sliding Mode Control*, Springer Berlin Heidelberg, pp. 21-53, 2013.

[23] R. Andreani, E. G. Birgin, J. M. Martnez, and M. L. Schuverdt, "On Augmented Lagrangian methods with general lower-level constraints," *SIAM Journal on Optimization*, vol. 18, no. 4, pp. 1286-1309, 2007.

[24] Z. Lin, M. Chen, and Y. Ma, "The Augmented Lagrange Multiplier Method for exact recovery of corrupted low-rank matrices," http://arxiv.org/abs/1009.5055.

[25] D. P. Bertsekas, *Constrained Optimization and Lagrange Multiplier Methods*, New York, USA: Academic Press, 1982.

[26] A. R. Conn, N. I. M. Gould, and P. L. Toint, *Trust region methods*, SIAM, 2000.